DexNet 1.0: Correlated Multi-Armed Bandit Models for Large Scale 3D Grasp Planning Under Uncertainty
v2 [2015-08-26 03:11]

Jeffrey Mahler, Brian Hou, Mel Roderick, Michael Laskey, Kai Kohlhoff,
Torsten Kroeger, Florian Pokorny, James Kuffner, Ken Goldberg

[TODO: POSSIBLY WILL INCLUDE MATTHIEU AUBRY AND PIETER ABBEEL AS COAUTHORS AS WELL]

***Abstract*— [TODO: FILL IN AFTER REST OF PAPER DONE.]**

I. Introduction

Robots in warehouse order fullfillment and small- to medium-scale manufacturing must be able to efficiently grasp and manipulate new products and parts. For example, a robot processing orders in a distribution warehouse must quickly plan graps for new consumer products to place them in shipping containers. Furthermore, a robot may not fully observe the state of the workspace, such as the pose or frictional properties of consumer products, due to sensor imprecision and missing data resulting from occlusions. This poses a challenge for grasp planning with either analytic methods [24], [17] that require precise knowledge of contact locations and surface normals or data-driven approaches [6] that attempt to build a statistical model of grasp success over the massive number of configurations of the environment.

Past work has attempted to overcome this by planning grasps analytically with high probability of force closure [45], [46], [50], [57], [78], or using data-driven methods to predict grasp success from human labels [2], [19], [34], [42], [53], [72] or empirical successes on a physical robot [7], [11], [21], [48], [62]. Many works on grasp selection with probablity of force closure evaluate a set of candidate grasps using sampling and select the highest quality grasp either using brute force sampling [45], [46], [78], iterative pruning [44], or Multi-Armed Bandit (MAB) algorithms to adaptively sample more promising grasps [3], [49], [50], [70]. However, MAB algorithms, the current fastest sampling method, still required approximately 10 samples per grasp to converge to a solution and needed to be re-run for every new object.

On the other hand, data-driven approaches have shown promise over analytic methods on physical robot trials [2], [34] possibly due to a reduction in modelling error. The number of objects and grasps tested is typically on the order of tens to hundreds for physical robot trials and at most a few thousand objects and hundreds of thousands of grasps when using simulation or human labels [30], [53], [42]. In comparison, state-of-the-art learning results in image classification [18], [47] and speech recognition [16], [32] relied on datasets containing tens of millions of examples.

Fig. 1: Sample of 3D mesh models from the DexNet dataset. The dataset consists of over 30,000 models from laser-scanned datsets such as the KIT object database [43] and the Yale-CMU-Berkeley object set [12], and synthetic datasets such as 3DNet[79] and the SHREC 2014 object retrieval challenge dataset [55]

This raises the question: will maching learning for grasp planning under vast numbers of possible object poses, object shapes, environment configurations, etc., exhibit scaling effects similar to those observed in computer vision and speech recognition?

To make progress toward answering this question, we introduce the Dexterity Network (DexNet) 1.0, a dataset of tens of thousands of 3D mesh models and a system for building statistical models that predict grasp quality across the dataset. DexNet is composed of laser-scanned 3D mesh models from the KIT object database [43], the Amazon Picking Challenge objects, BigBIRD [73], and YCB [12], and synthetic 3D mesh models from 3DNet [79] and the SHREC 2014 large scale object retrieval challenge [55]. Fig. 1 shows a subset of the objects in the dataset. To measure similarity between objects, we form an object network based on Deep Convolutional Neural Networks (CNNs) trained to predict object categories from synthetic rendered images of each object [1], [55]. The DexNet system uses Google Compute Engine to launch up to 600 instances at a time to samples and evaluate grasps on subsets of objects and to learn predictive models of grasp quality.

In this work, we use DexNet to study the number of samples that MAB algorithms take to converge to a grasp with high probability of force closure across orders of magnitude of prior data of grasps with known quality. To do so, we extend the MAB framework of Laskey et al. [50] to model correlations between the probability of force closure for grasps on similar objects using Continuous Correlated Beta Processes (CCBPs) [27], [62]. CCBPs allow us to form a prior belief on the quality of candidate grasps for a new object based on data in DexNet and to efficiently update

a global belief on the quality of all candidate grasps on an object after observing the outcome of a single sampled grasp. We measure local similarities between grasps on the same object by a distance between the gripper poses and the similarity between local surface patches near the mean location of contact on the object [34], [42]. We measure global similarity in shape based on the distance between the objects in DexNet. Our results suggest [TODO: FILL IN WITH NEW RESULTS].

II. Related Work

Many works on grasp planning focus on finding grasps by maximizing a grasp quality metric, such as the ability to resist external perturbations to the object in wrench space [24], [61]. These metrics have been used to synthesize grasps for known objects using sampling-based optimization in software tools such as GraspIt! [61] or OpenGRASP [54]. However, analytic grasp quality metrics have been criticized for relying on perfect knowledge of object shape, pose, material properties, and locations of contact [13], [22], [78], [80] and for not taking into account the dynamics of the the grasp [4], [65]. Recent work has also suggested that grasp closure metrics may fail to accurately predict of grasp success on a physical robot [2], [78]. This has motivated work on transferring known grasps from a database to new objects, evaluating robust versions of analytic quality metrics with respect to uncertainty in the state of the robot and environment, and work on data-driven grasp synthesis.

Many works have approached grasp synthesis for unknown or familiar objects by transferring grasps from a benchmark set of exemplar objects in a large database. Li and Pollard [56] generated grasps by matching object shapes to human hand postured in a database. Goldfelder et al. [30] developed the Columbia grasp database, a database of 1,814 distinct models and over 200,000 form closure grasps generated using the Eigengrasp planner in GraspIt! [17]. The authors later used synthetic partial depth maps of objects in the database to match robot sensor data to precomputed grasps, using the Iterated Closest Point (ICP) algorithm to align the coordinate frames of the depth maps [31], [29]. Several works have also transferred grasps from objects of the same category by warping contacts betwen corresponding points on a shape surface and locally replanning using local rigid alignment and contact interpolation [35], [74] or by interpolating a shape and grasp over a Grasp Moduli Space [64], [63]. Detry et al. [20] create a low-dimensional representation of object parts and cluster object parts that are grasped similarly to form a shape library of prototypical grasp parts, and show that this representation can be transferred to real sensor data [19].

Work on evaluating grasp quality metrics under uncertainty, such as the probability of force closure, has considered uncertainty in the state of a robotic gripper [28], [75] and uncertainty in contact locations with an object [80]. Recent work has also studied the effects of uncertainty in object pose and gripper positioning [11], [37]. Brook, Ciocarlie, and Hsiao [11], [37] studied a Bayesian framework to evaluate the probability of grasp success given uncertainty in object identity, gripper positioning, and pose by simulating grasps on deterministic mesh and point cloud models. Weisz et al. [78] and Kim et al. [46] independently found that grasps ranked by probability of force closure subject to perturbations of object pose in simulation were empirically more successful on a physical robot than grasps planned using deterministic wrench space metrics. Many works have also studied grasping under object shape uncertainty resulting from imprecision of object segmentations in images [14], part tolerancing in manufacturing [44], [45], or missing and noisy data from depth sensors such as the Kinect modeled with Gaussian process implicit surfaces [57], [50]. Many have also studied caging gripper configurations [69], which are a waypoint to form closure grasps for two fingers [76], [71] and may be robust to perturbations in object pose and shape [23], [77].

Another approach for synthesizing grasps on objects is to sample grasps and rank them according to metrics derived from human labels or physical execution [6]. Saxena et al. [40], [72] used a logistic regression classified to predict grasp afordances in images from human annotated training data. Several other works have examined predicting grasp points using depth edges [66], combinations of 2D and 3D edges [52], and global shape descriptors [5]. Lenz et al [53] used deep learning to detect grasp bounding boxes in color and depth images, which was later extended to real time by Redmon and Angelova [68]. Many works have also considered predicting grasp success from 3D point clouds. Herzog et al. [33], [34] extract ”heightmaps” of local object curvature from human demonstrated grasps, construct a library of heightmap templates, and match new sensor data to templates to select grasps similar to the demonstrations. Kappler et al. [42] trained a deep neural network to predict human labelled grasps for a Barett hand on a database of synthetic pointclouds of objects. Recently, several other works have proposed to form a huge database of grasps on synthetic objects from simulation outcomes [60] or physical execution [**?**]. In comparison, our work studies the convergence rate for adaptively acquiring samples for evaluating and ranking grasps by their likelihood of success through the use of data-driven grasp correlations based on local and global features of an object surface.

Many works have also considered using data-driven approaches for actively selecting grasps. Several works have studied active search for successful grasps by minimzing uncertainty about the state of the envirnoment [38], [41], [25], but without use of an explicit grasp quality metric to guide the search. Kehoe et al. [44] proposed iterative pruning, an algorithm for evaluating the probability of force closure for a set of candidate grasps while discrading grasps known to have poor quality. Tellex et al. [] proposed an initiative to adaptively collect a dataset of grasps and point clouds for one million objects using MAB and reinforcemen learning. Detry et al. [21] estimated a full continuous density function over grasp poses using kernel density estimation and adaptively acquired samples by pruning unsuccessful grasps.

Recently, Laskey et al. [50] showed that Multi-Armed Bandit algorithms can be used to accelerate the identification of grasps with high probability of force closure under uncertainty in shape, pose, and friction in 2D over candidate sets of 1,000 grasps on 88 objects. MAB algorithms select the next grasp to sample by trading off gaining information about grasps with few samples and exploiting the success of grasps known to work well. In robotics, MAB algorithms have also been for speeding up probabilistic roadmap motion planning by adaptively sampling waypoints [39], searching for the best state machine for a particular task [59], solving mixed observable POMDPs [51], and multi-agent navigation [26].

One shortcoming of the MAB model used by Laskey et al. is that it did not take into account correlations between grasps [50]. In reality, grasp correlations may occur from grasps with similar configurations [17], [21], objects with similar global structure [64], or on point cloud surfaces with similar local geometry [9], [33], [48], [72]. Correlated Multi-Armed Bandit (CMAB) models, sometimes also referred to as Bayesian Optimization models [10], have been used to trading off infromation gathering and exploitation in applicatoins such as ad-serving [15] and envrionmental monitoring in robotics [36], [58]. Perhaps the most common model of correlations in a CMAB is a linear model [15], however this depends on the selection of features are linearly related to a success criteria. Another common model of correlations is a Gaussian Process (GP) [67], which can model non-linear relationships between options and rewards. Kroemer et al. [48] developed a reinforcement learning approach to grasp selection based on seeding hypothesse via imitation learning and Gaussian process upper-confidence bounds to predict grasp successeses and determine the next grasp to select. Boularias et al. [7] used a Gaussian process Bayesian Optimization model for selecting grasps on cluttered piles of rocks. However, GP models are expensive to update with new observations ($O(n^2)$ where n is the number of observations so far) [67], which limited the scale of experiments in both simulation and the physical world that the authors could perform. To make the model more tractable, Boularias et al. later extended their work to use an heuristic upper confidence bound-based reinforcement learning [8]. Recently, Goetschalckx et al. [27] developed the Continuous Correlated Beta Process (CCBP), a nonlinear model of 0-1 reward probabilities. CCBPs are inexpensive to update compared to GPs, requiring $O(n)$ time in the worst case and a much smaller factor when approximate kernels are computed using efficient nearest neighbor queries [27]. Montesano and Lopes [62] used CCBPs (although the authors did not refer to them as CCBPs) to actively acquire grasp executions, measuring correlations from the responses to a bank of 151 image filters. In this work we also utilize CCBPs to model correaltions between grasps, and study their performance on grasping simulations over thousands of objects.

III. Definitions and Problem Statement

We consider the problem of finding the parallel-jaw grasp with the maximum probability of a binary success metricsuch as force closure on a previously unknown object under uncertainty in object pose, gripper pose, and friction coefficient.

(a) Grasp Parameterization (b) Contact Model

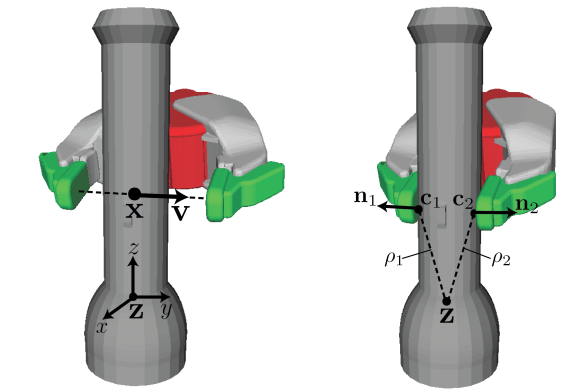

Fig. 2: (Left) We parameterize parallel-jaw grasps by the centroid of the jaws $\mathbf{x} \in \mathbb{R}^3$ and approach direction, or direction along which the jaws close, $\mathbf{v} \in \mathcal{S}^2$. The grasp parameters $\mathbf{x}$ and $\mathbf{v}$ are specified with respect to a coordinate frame located at the object center of mass $\mathbf{z}$ and oriented along the principal directions of the object. (Right) The jaws are closed until contacting the object surface at locations $\mathbf{c}_1, \mathbf{c}_2 \in \mathbb{R}^3$, at which the surface has normals $\mathbf{n}_1, \mathbf{n}_2 \in \mathbb{S}^2$. The contacts are used to compute the moment arms $\rho_1 = \mathbf{c}_1 - \mathbf{z}$ and $\rho_2 = \mathbf{c}_2 - \mathbf{z}$. From these parameters we can derive the theoretical forces and torques that the gripper can apply to the object.

A. Grasp and Object Model

Our grasping model is illustrated in Fig. 2. Let $\mathbf{g} = [\mathbf{x}, \mathbf{w}]^T$ be a parallel-jaw grasp parameterized by the centroid of the jaws in 3D space $\mathbf{x} \in \mathbb{R}^3$ and an approach direction, or axis, $\mathbf{v} \in \mathcal{S}^2$. We assume that the gripper will be opened to its maximal width before closing on the object. Let $f : \mathbb{R}^3 \rightarrow \mathbb{R}$ be a signed distance function (SDF) representing an object's geometry [**?**], [57], which is zero on the object surface, positive outside the object, and zero inside the object. We assume that the object is specified in units of meters and the object center of mass $\mathbf{z} \in \mathbb{R}^3$ is known. Let $\mathcal{G} = \{[\mathbf{x}, \mathbf{w}]^T \big| \mathbf{x} \in \mathbb{R}^3, \mathbf{v} \in \mathcal{S}^2\}$ denote the space of all grasps and $\mathcal{H} = \{\mathcal{O} = \{\mathbf{z}, f(\cdot)\} \big| \mathbf{z} \in \mathbb{R}^3, f \in \mathcal{F}\}$ denote the space of all objects, where $\mathcal{F}$ is the space of all SDFs. Our joint grasp and object space, or Grasp Moduli Space [64], is $\mathcal{M} = \mathcal{G} \times \mathcal{H}$.

B. Sources of Uncertainty

We assume known uncertainty in object pose, gripper pose, and friction coefficient resulting from sensing uncertainties and missing data following the model of Laskey et al. [50]. Let ξ be Gaussian uncertainty in object pose with mean $\bar{T} \in SE(3)$ and covariance Σ_ξ following the model of Barfoot and Furgale [**?**]. Let ν be uncertainty in gripper pose distributed as a Gaussian with mean $\mu_\nu \in \mathcal{G}$ and covariance Σ_ν. Let γ denote uncertiainty in friction coefficient distributed as a Gaussian with mean $\mu_\gamma \in \mathbb{R}$ and covariance Σ_γ. Theses sources of uncertainty might be estimated based on prior models of repeatability in gripper actuation or from the posterior variance in object pose or friction coefficient in estimates based on sensor data.

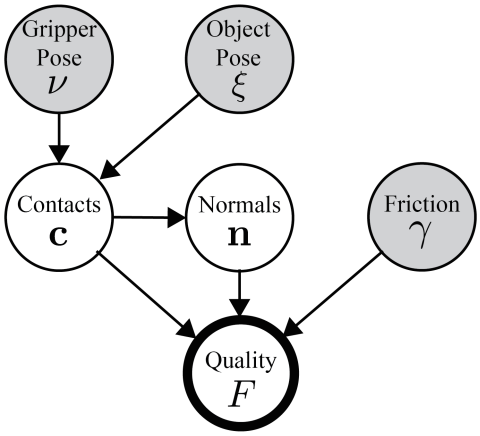

Fig. 3: A graphical model describing the relationships between known uncertain parameters (shaded gray) such as object pose and the force closure random variable F.

C. Contact Model

Our contact model is illustrated in the right panel of Fig. 2. Given object shape and samples of object pose, and gripper pose, we let $\mathbf{c}_i \in \mathbb{R}^3$ for $i \in 1, 2$ denote the 3D location of contact between the i-th gripper jaw and surface. Furthermore, let $\mathbf{n}_i \in \mathcal{S}^2$ denote the surface normal at contact $\mathbf{c}_i$. To compute the forces that each contact can apply to the object, we discretize the friction cone at contact i into a discrete set of N_c facets with vertices $\mathbf{f}_{i,j}$ for $j = 1, ..., N_c$ [**?**] for a given friction coefficient γ. Each force $\mathbf{f}_{i,j}$ can exert a corresponding torque $\tau_{i,j} = \mathbf{f}_{i,j} \times \rho_i$ where $\rho_i = (\mathbf{c}_i - \mathbf{z})$ is the moment arm at contact i. Thus the set of all wrenches that can be applied by a grasp $\mathbf{g}$ is $\mathcal{W} = \{\mathbf{w}_{i,j} = [\mathbf{f}_{i,j}, \tau_{i,j}]^T | i = 1, 2 \text{ and } j = 1, ..., N_c\}$.

D. Quality Metric

In this work we use force closure, or the ability to resist external force and torques in arbitrary directions [24], as our grasp success metric. We acknowledge that force closure assumes the abliity to actuate the gripper to apply arbitrary forces in the contact friction cone [] and that some evidence suggests that deterministic force closure is not a strong predictor of physical grasp success [2]. However, we use the probability of force closure because of it has shown some promise in physical experiments [46], [78], and it is relatively inexpensive to evaluate as compared to human labels or physical executions, allowing us to better study the effects of large amounts of data on convergence.

Let $F \in \{0, 1\}$ denote the occurence of force clsoure. To compute force closure for a grasp $\mathbf{g}$ on object $\mathcal{O}$ given deterministic samples of object pose ξ, gripper pose ν, and friction coefficient γ, we first compute the set of possible contact wrenches $\mathcal{W}$. Then $F = 1$ if the origin lies within the convex hull of the contact wrench set, $\mathbf{0} \in Conv(\mathcal{W})$. A graphical model describing the relationship between these quantities is given in Fig. 3.

E. Objective

The probability of force closure for a grasp $\mathbf{g}$ is

$$P_F(\mathbf{g}) = \mathbb{P}\left(F = 1 \mid \mathbf{g}, \mathcal{O}, \xi, \rho, \zeta\right).$$

We are interested in finding the candidate grasp that maximizes the probability of force closure $P_F(g)$ [46], [50], [57], [78] subject to these sources of uncertainty over a budgeted maximum number of samples T. To perform this as q uickly as possible we formulate this as a maximization over the sum of the true P_F for the grasps sampled at iteration t, where $I(i)$ denotes the grasp selected at time t:

$$\underset{g_{I(1)},\ldots,g_{I(T)} \in \mathcal{G}}{\text{maximize}} \sum_{t=1}^{T} P_F(g_{I(t)}). \tag{III.1}$$

As the maximization over the continuous space $\mathcal{G}$ is computationally expensive, past work has solved this objective using a discrete set of K candidate grasps $\Gamma = \{\mathbf{g}_1, ..., \mathbf{g}_K\}$ where Γ is set using Gaussian sampling of grasp centers and poses [50] or using heuristics such as antipodality [**?**]. However, even with a discrete set of candidates, fully evaluating $P_F(\mathbf{g})$ for any grasp requires an expensive integration over possible contact locations between the grasp and surface and the surface normals at these contacts [57]. Thus, past work has evaluated the probability of force closure using Monte-Carlo integration [44], [45], [78], approximating the expression by minimzing uncertainty at the contact locations [57], and using Multi-Armed Bandit algorithms to jointly evaluate $P_F(\mathbf{g})$ using Monte-Carlo integration while allocating samples to more promising grasps. In this work, we propose to use Multi-Armed Bandits with correlations between arms to further accelerate convergence.

[TODO: SWITCH TO TASK-BASED QUALITY METRIC (E.G. RESITING GRAVITY)? I THINK IT WOULD BE MORE COMPELLING BUT DOESN'T SEEM TO HAVE MUCH PRECEDENT UNDER UNCERTAINTY]

IV. Correlated Multi-Armed Bandit Model

Finding an approximate solution of Equation III.1 using Multi-Armed Bandits requires a predictive model of the probability of force closure for each grasp. We use Continuous Correlated Beta Processes (CCBPs) to model force closure for a grasp as a Bernoulli random variable with correlations across grasps and objects [27], [62]. Fig. **??** illustrates how using a correlated model can lead to accelerated convergence of bandit algorithms.

A. Continuous Correlated Beta Processes

Continuous Correlated Beta Processes(CCBPs) were independently developed by Goetschalckx et al. [27] and Montesano and Lopes [62] to model correlations between the Bernoulli random variables in a Beta-Bernoulli process, which may lead to faster convergence in Multi-Armed Bandit problems [15]. Such correlations may exist when the Bernoulli random variables depend on common latent factors. For example, two probability of force closure variables θ_k may be correlated when two grasps contact the same

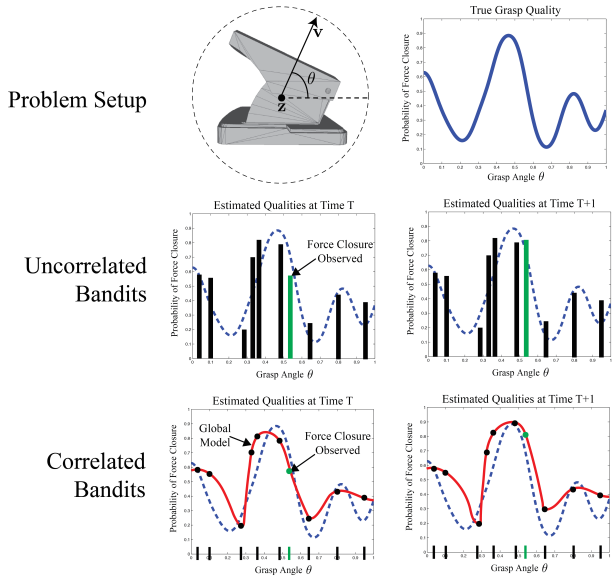

Fig. 4: (Top Left) Consider a set of grasps with fixed center at an object center of mass and approach direction sampled along a one-dimensional circle. (Top Right) The true probability of force closure P_F may vary smoothly as a function of the angle of the grasp axis. (Middle Left) Uncorrelated MAB models maintain an estimate of P_F independently for each grasp, indicated by bars and their height. On iteration T of a MAB algorithm, the grasp indicated with a green bar is sampled and returns force closure. (Middle Right) Only the estimate of P_F for the sampled grasp is updated for iteration $T+1$, and the grasp with highest estimated P_F remains suboptimal. (Bottom Left) Correlated MAB models maintain a global predictive function (in red) of P_F for any possible grasp but may select grasps from a set of discrete candidates (indicated by dots). (Bottom Right) On iteration $T+1$ the grasp indicated by the green dot again returns force closure and the global model is updated, increasing the estimated P_F for "nearby" grasps. Although a suboptimal grasp was sampled, the global model now correctly predicts the optimal grasp in the set.

shape in similar locations or when grasps on different shapes have similar local surface geometries, such as grasping the handle of a mug and the handle of a teapot

Let $\Gamma = \{\mathbf{g}_k\}_{k=1}^K$ denote our discrete set of K candidate grasps for object $\mathcal{O}$. Let $F(\mathbf{g}_k) \in \{0,1\}$ denote the occurence of force closure for a grasp $\mathbf{g}_k$. We model $F(\mathbf{g}_k)$ as a Bernoulli random variable with probability of success $\theta_k = P_F(\mathbf{g}_k)$. Since we do not know the value of θ_k for each grasp, we maintain a belief distribution for each θ_k based on our prior belief about the likelihood of force closure. A common choice for a belief distribution on the Bernoulli parameter θ_k is the Beta distribution, which is specified by shape parameters $\alpha > 0$ and $\beta > 0$:

$$\text{Beta}(\alpha,\beta) = \frac{1}{B(\alpha,\beta)}\theta_k^{\alpha-1}(1-\theta_k)^{\beta-1}$$

A CCBP estimates the shape parameters for a grasp $\mathbf{g}$ on object $\mathcal{O}$ using a normalized kernel function $k(\mathbf{y}_i,\mathbf{y}_j) : \mathcal{M}\times\mathcal{M} \to [0,1]$ that measures similarity between two elements of the Grasp Moduli Space, where $\mathbf{y} = \{\mathbf{g},\mathcal{O}\} \in \mathcal{M}$. The kernel approaches 1 as the arguments become increasingly similar and approaches 0 as the arguments become dissimilar. In this work we use a unit-bandwidth squared exponential kernel

$$k(\mathbf{y}_i,\mathbf{y}_j) = \exp\left(-\frac{1}{2}\sum_{m=1}^{N_f} w_m^2 \|\varphi_m(\mathbf{y}_i) - \varphi_m(\mathbf{y}_j)\|_2^2\right)$$

where $\varphi_m : \mathcal{M} \to \mathbb{R}^{d_m}$ for $m = 1,...,N_f$ are feature mappings for a grasp and object to a d_m-dimensional Euclidean space and $w_m \in \mathbb{R}$ are weights scaling the relative contribution of the feature maps to the similarity metric.

Upon observing force closure for a grasp and object, we update the Beta belief for every other grasp proportional to how similar it is to the observed grasp as measured by the kernel. Let $F_1(\mathbf{g}_{I(1)}),...,F_t(\mathbf{g}_{I(t)})$ be t sequential observations of force closure from samples of our uncertainty models for grasps $\mathbf{g}_{I(1)},...,\mathbf{g}_{I(t)}$, where $I(j)$ is the index of the grasp sampled at time j. Then the CCBP posterior update for θ_k is [27]:

$$p\left(\theta_k | F_1(\mathbf{g}_{I(1)}),...,F_t(\mathbf{g}_{I(t)})\right) = \text{Beta}\left(\alpha_{k,t},\beta_{k,t}\right)$$

$$\alpha_{k,t} = \alpha_{k,0} + \sum_{j=1}^{t} k(\mathbf{y}_k,\mathbf{y}_{I(j)})F_i(\mathbf{g}_{I(j)}) \tag{IV.1}$$

$$\beta_{k,t} = \beta_{k,0} + \sum_{=1}^{t} k(g\mathbf{y}_k,\mathbf{y}_{I(j)})(1-F_i(\mathbf{g}_{I(j)})) \tag{IV.2}$$

Intuitively, this allows observations of one grasp to constitute fractional observations of similar grasps.

B. Feature Mappings

We use feature mappings $\varphi_1,...,\varphi_{N_f}$ that capture both lsimilarity based on local surface geometry and grasp parameters and global object shape.

1) Local Features: Since grasps may be correlated across very small changes to the grasp center and approach direction on a single shape, our first feature map $\varphi_\ell(\mathbf{y}) = \mathbf{g}$ is the identity transformation for the grasp. However, similarity between grasp centers and approach directions does not indicate similar P_F if the two surfaces are dissimilar. For example, two grasps contacting a box on opposite sides of a corner may be very similar according to φ_ℓ but likely to contact the object on surfaces with very different orientations.

To mitigate this issue, we use a variant of the grasp heightmap features of Herzog et al. [33] and Kappler et al. [42]. In this work, we capture local surface patches by an image oriented along a tangent plane to the grasp axis at a contact point, where each pixel stores the distance from the pixel center on the plane to the surface along the grasp axis. Let $d_g \in \mathbb{Z}$ be the number of pixels along each dimension of the heightmap, let $\delta \in \mathbb{R}$ be the resolution of the image pixels in meters, and let $r \in \mathbb{R}$ be a minimum projection distance. Furthermore, let $\mathbf{c}_k, k = 1,2$ be a contact point for grasp $\mathbf{g}$ and let $\mathbf{t}_1,\mathbf{t}_2$ be two orthogonal vectors to the grasp approach direction $\mathbf{v}$. Then to compute the heightmap value at pixel (i,j) we first compute the 3D location of the pixel on the plane, $\mathbf{p}_k(i,j) = \mathbf{c}_k + i\delta\mathbf{t}_1 + j\delta\mathbf{t}_2$. Then we

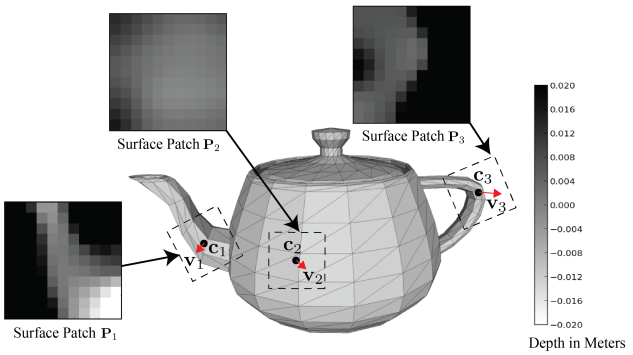

Fig. 5: Three local surface heightmaps extracted on a teapot. Each heightmap is "rendered" along the grasp axis at each contact point and oriented by the local directions of maximum variation in the heightmap.

assign the heightmap value $\mathbf{h}_k(i,j) = t^*$, where t^* is the smallest value of $t > -r$ such that $\mathbf{p}_k(i,j) + t\mathbf{v}$ contacts the shape surface. Finally, we rotate the heightmap to align the axes with the eigenvectors of a weighted covariance matrix as in [**?**] in order to make our feature representation rotationally invariant. Our feature vector for the heightmaps is $\varphi_h(\mathbf{g}_i, \mathcal{O}_i) = [\mathbf{h}_1, \mathbf{h}_2]^T$. Fig. 5 illustrates local surface patches extracted by this procedure.

2) Global Features: Purely local features may not capture all correlations in probability of force closure between pairs of grasps and objects. For example, grasps on the handle of a teapot may have similar grasp center, grasp axis, and even local surface geometry to another tubelike object such as a pen, but different P_F. To measure global shape similarity, we develop a novel viewpoint-based object representation that pools the views from many virtual viewpoints rendered on a sphere surrounding the object.

[TODO: JUSTIFY WHY CLASS LABELS HELP, IF THEY DO]

Fig. 6 illustrates our method. We first render every object to 50 virtual cameras discretized along equal angle increments and oriented toward the object center using Maya. Then we finetune AlexNet [47], a common deep Convolutional Neural Network (CNN) architecture, to predict a class label for each image based on known class labels for the 3D models. Next, we pass each of the 50 views of each object through the finetuned CNN and max-pool the output of the fc7 layer. As the output is nearly 400 dimensions, we finally reduce the max-pooled output to 100 dimensions using Principal Component Analysis (PCA). This yields a representation $\psi(\mathcal{O}) \in \mathbb{R}^{100}$ for each object.

[TODO: EXPAND ABOVE PARAGRAPH, INCLUDE MORE DETAILS ON METHOD AS WELL AS THE RESULTS OF TRAINING]

C. Optimizing Feature Weights

One remaining issue is the selection of the relative feature weights $w_1, ..., w_{N_f}$. Past work has optimized these weights using a squared error loss on the probability of success predicted by the CCBP and a true probability of success from brute force evaluation [62]. However, this criterion may be inappropriate for predicting probabilities, as the predictions must be bounded between 0 and 1. In this work we instead select the weights which minimze the cross entropy loss []:

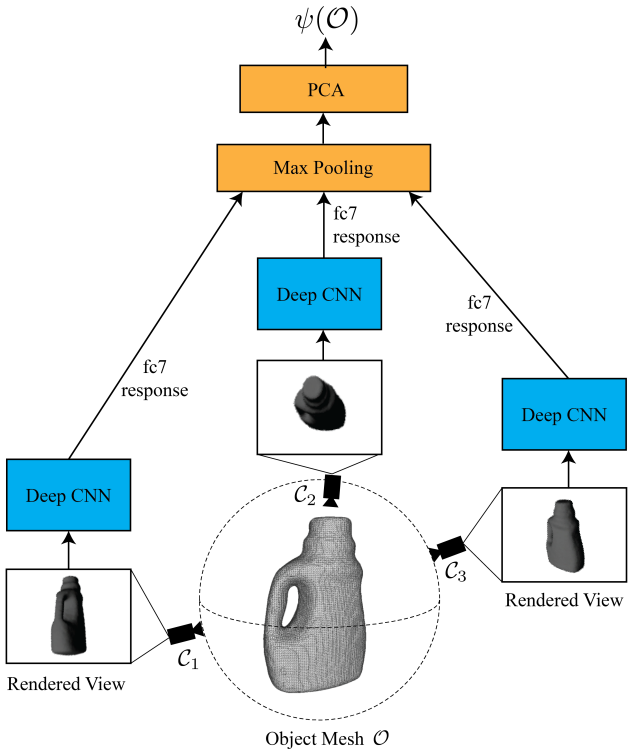

Fig. 6: Illustration of our method for embedding 3D object models in a Euclidean vector space for computing global shape similiarty. We pass a set of 50 virtually rendered camera viewpoints discretized around a sphere through a deep Convolutional Neural Network (CNN) with the AlexNet [47] architecture. Finally, we take the maximum fc7 response across each of the 50 views for each dimension and run PCA to reduce the dimensionality of the output.

$$w_1^*, ..., w_{N_f}^* = \underset{w_1 \geqslant 0, ..., w_{N_f} \geqslant 0}{\operatorname{argmin}} \frac{1}{M} \sum_{i=1}^{M} \mu_i \log\left(\frac{\alpha_i}{\alpha_i + \beta_i}\right) + (1 - \mu_i) \log\left(\frac{\beta_i}{\alpha_i + \beta_i}\right)$$

where α_i and β_i are the posterior shape parameters given by Equations IV.1 and IV.2 and μ_i is the known probability of force closure evaluated by exhaustive Monte-Carlo integration for a set of M grasps. We optimize this objective using Stochastic Gradient Descent (SGD) with the weights all initialized to 100.

V. Algorithm

[TODO: BRIEF SECTION ON THE HIGH-LEVEL ALGORITHM USING THE MODEL: GRASP SAMPLING, EVALUATION OF GRASPS, THOMPSON SAMPLING]

VI. Experiments

A. Dataset

To study the convergence rate with orders of magnitude of previous grasp data we create a dataset of tens of thousands of 3D CAD models. We aggregated data from the laser scanned datasets Amazon Picking Challenge [], BigBIRD [], KIT [], and YCB [], as well as the synthetic

datasets 3DNet [79] and the SHREC 2014 large-scale retrieval dataset []. To preprocess the data for grasping we set the frame of reference for each object to the the principal components of the vertices of each mesh, set the object center-of-mass as the center of a bounding box around the reoriented vertices, removed unreferenced and invalid vertices, rescaled each synthetic mesh such that its smallest principal direction fit within a PR2 gripper, and converted the mesh to a signed distance field. We reserved the YCB dataset as a test set, and used subsets of the remaining data to train hyperparameters and to seed the CCBPs for convergence experiments on the test dataset.

B. System

To handle the scale of the experiments, we developed a Cloud-based software library on top of Google Cloud services. We used Google Cloud Storage (GCS) to store the mesh models and to sample and evaluate 250 grasps per object. Each model is stored in .OBJ format and the average size is roughly 0.5MB. We used Google Compute Engine to distribute trials of MAB algorithms across objects, reducing the runtime of our large-scale experiments. Our master analysis script can launch up to 600 GCE single core instances, each running Ubuntu 12.04. When an instance is launched, we mount DexNet via a persistent disk containing a particular set of objects and grasps. Each instance pulls our latest code from Github, runs a single python experiment script configured in a YAML file, compresses the results in an output directory, and uploads the results to GCS. After all instances complete, the master script turns off all instances, unmounts all disks, downloads the results from each instance, and sends the user a notification email. The results can be optionally analyzed by the master script.

C. Rate of Convergence

[TODO: REPLACE WITH FINAL VERSIONS. THE CURRENT RESULTS ARE PRELIMINARY]

Preliminary experiments suggest that using CCBPs with prior data from DexNet reduces the number of samples for MAB algorithms to converge to a grasp with high probablity of force closure P_F under uncertainty in object pose, gripper pose, and friction coefficient. Fig. 7 shows the normalized P_F (the ratio of the P_F for the sampled grasp to the P_F in the candidate grasp set) versus iteration averaged over 20 trials for a cereal box and flower pot. The plot compares Thompson sampling, a MAB algorithm, without correlations to Thompson sampling using the CCBP model of local grasp similiarity (no prior data). We see that the CCBP model outperforms the uncorrelated model by approximately $10\times$ for the cereal box but has comparable performance to Thompson sampling on the flower pot. Iniitial reuslts suggest that performance on the flower pot is poorer because it has very few similar grasps according to our similarity metric.

To examine the effects of orders of magnitude of prior data in the MAB algorithms, we ran the algorithms with priors computed from increasingly larger subsets of prior data from DexNet: 0, 15, 150, and 1500 objects. Fig. 8 shows the

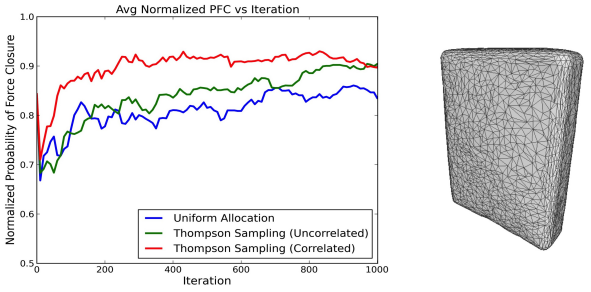

(a) Normalized P_F on a cereal box with 250 candidate grasps.

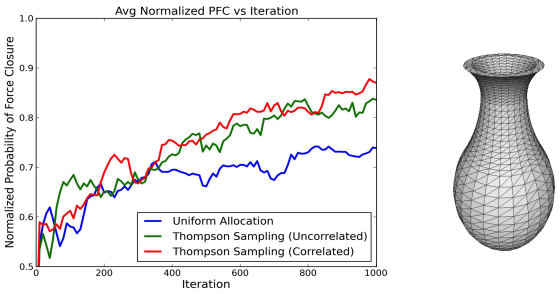

(b) Normalized P_F on a flower pot with 250 candidate grasps.

Fig. 7: Comparison of the normalized P_F of the sampled grasp versus iteration of the MAB algorithm for correlated Thompson sampling, uncorrelated Thompson sampling, and Uniform Allocation averaged over 20 trials. (a) On the cereal box, correlated Thompson sampling converges to within 90% of the highest quality grasp approximately $4\times$ faster than uncorrelated. (b) However, correlated and uncorrelated Thompson sampling perform comparably on the flower pot because there are few grasp similarities in the candidate set.

normalized probability of force closure P_F versus iteration when planning grasps for a bottle using prior grasp data from the five nearest neighbor objects in DexNet averaged over 50 trials. Each other object was labelled with 250 grasps and P_F evaluated using brute force Monte-Carlo integration. We see that the convergence of the correlated MAB algorithms to a grasp with high P_F accelerates with increasingly largers subsets of prior data used. This suggests that adding more prior data may further accelerate convergence, because it is increasingly likely that a similar object and grasp exists in the dataset as the size increases. Future work will examine these effects on a larger subset of objects and will use more than five nearest neighbors from DexNet to compute priors, which may lead to even larger gains for larger subsets of prior data.

[TODO: REMOVE BELOW SECTION] We are currently working on an experiment to quantify the gains in convergence time across orders of magnitudes of prior data (10, 100, 1000, 10000) from DexNet using Google Compute Engine. Our initial version will be run on a relatively small subset of test objects, and in the coming weeks we will average the performance over a larger set of test objects. We are particularly interested in seeing if there is a point of diminishing returns from adding more data when using datasets on the order of 10,000 - 100,000 objects. We are also interested in whether or not adding perturbations to the data such as object reflections and shape perturbations will also increase performance, as has been observed for training

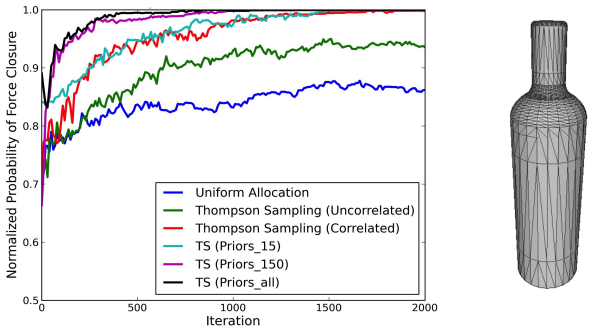

Fig. 8: Comparison of the normalized P_F of the sampled grasp (y-axis) versus iteration of the MAB algorithm (x-axis) for correlated Thompson sampling with and without the use of prior grasps from five nearest neighbors from DexNet, uncorrelated Thompson sampling, and Uniform Allocation averaged over 20 trials on the bottle object. Prior grasps were taken from increasingly larger subsets of DexNet: 15, 150, and 1500 objects. We see that convergence to within 90% of the optimal grasp is accelerated by approximately $10\times$ over uncorrelated Thompson sampling, and performance appears to improve with increasing sizes of the prior dataset used.

Deep CNNs in vision [47].

VII. Sensitivity to Uncertainty

References

[1] M. Aubry and B. Russell, "Understanding deep features with computer-generated imagery," *arXiv preprint arXiv:1506.01151*, 2015.

[2] R. Balasubramanian, L. Xu, P. D. Brook, J. R. Smith, and Y. Matsuoka, "Physical human interactive guidance: Identifying grasping principles from human-planned grasps," *Robotics, IEEE Transactions on*, vol. 28, no. 4, pp. 899–910, 2012.

[3] A. G. Barto, *Reinforcement learning: An introduction*. MIT press, 1998.

[4] A. Bicchi and V. Kumar, "Robotic grasping and contact: A review," in *ICRA*. Citeseer, 2000, pp. 348–353.

[5] J. Bohg and D. Kragic, "Learning grasping points with shape context," *Robotics and Autonomous Systems*, vol. 58, no. 4, pp. 362–377, 2010.

[6] J. Bohg, A. Morales, T. Asfour, and D. Kragic, "Data-driven grasp synthesisa survey," *Robotics, IEEE Transactions on*, vol. 30, no. 2, pp. 289–309, 2014.

[7] A. Boularias, J. A. Bagnell, and A. Stentz, "Efficient optimization for autonomous robotic manipulation of natural objects," 2014.

[8] ——, "Learning to manipulate unknown objects in clutter by reinforcement," in *Twenty-Ninth AAAI Conference on Artificial Intelligence*, 2015.

[9] A. Boularias, O. Kroemer, and J. Peters, "Learning robot grasping from 3-d images with markov random fields," in *Intelligent Robots and Systems (IROS), 2011 IEEE/RSJ International Conference on*. IEEE, 2011, pp. 1548–1553.

[10] E. Brochu, V. M. Cora, and N. De Freitas, "A tutorial on bayesian optimization of expensive cost functions, with application to active user modeling and hierarchical reinforcement learning," *arXiv preprint arXiv:1012.2599*, 2010.

[11] P. Brook, M. Ciocarlie, and K. Hsiao, "Collaborative grasp planning with multiple object representations," in *Proc. IEEE Int. Conf. Robotics and Automation (ICRA)*. IEEE, 2011, pp. 2851–2858.

[12] B. Calli, A. Walsman, A. Singh, S. Srinivasa, P. Abbeel, and A. M. Dollar, "Benchmarking in manipulation research: The ycb object and model set and benchmarking protocols," *arXiv preprint arXiv:1502.03143*, 2015.

[13] J.-S. Cheong, H. Kruger, and A. F. van der Stappen, "Output-sensitive computation of force-closure grasps of a semi-algebraic object," vol. 8, no. 3, pp. 495–505, 2011.

[14] V. N. Christopoulos and P. Schrater, "Handling shape and contact location uncertainty in grasping two-dimensional planar objects," in *Intelligent Robots and Systems, 2007. IROS 2007. IEEE/RSJ International Conference on*. IEEE, 2007, pp. 1557–1563.

[15] W. Chu, L. Li, L. Reyzin, and R. E. Schapire, "Contextual bandits with linear payoff functions," in *International Conference on Artificial Intelligence and Statistics*, 2011, pp. 208–214.

[16] C. Cieri, D. Miller, and K. Walker, "The fisher corpus: a resource for the next generations of speech-to-text." in *LREC*, vol. 4, 2004, pp. 69–71.

[17] M. T. Ciocarlie and P. K. Allen, "Hand posture subspaces for dexterous robotic grasping," *Int. J. Robotics Research (IJRR)*, vol. 28, no. 7, pp. 851–867, 2009.

[18] J. Deng, W. Dong, R. Socher, L.-J. Li, K. Li, and L. Fei-Fei, "Imagenet: A large-scale hierarchical image database," in *Computer Vision and Pattern Recognition, 2009. CVPR 2009. IEEE Conference on*. IEEE, 2009, pp. 248–255.

[19] R. Detry, C. H. Ek, M. Madry, and D. Kragic, "Learning a dictionary of prototypical grasp-predicting parts from grasping experience," in *Robotics and Automation (ICRA), 2013 IEEE International Conference on*. IEEE, 2013, pp. 601–608.

[20] R. Detry, C. H. Ek, M. Madry, J. Piater, and D. Kragic, "Generalizing grasps across partly similar objects," in *Robotics and Automation (ICRA), 2012 IEEE International Conference on*. IEEE, 2012, pp. 3791–3797.

[21] R. Detry, D. Kraft, O. Kroemer, L. Bodenhagen, J. Peters, N. Krüger, and J. Piater, "Learning grasp affordance densities," *Paladyn, Journal of Behavioral Robotics*, vol. 2, no. 1, pp. 1–17, 2011.

[22] R. Diankov, "Automated construction of robotic manipulation programs," Ph.D. dissertation, Citeseer, 2010.

[23] R. Diankov, S. S. Srinivasa, D. Ferguson, and J. Kuffner, "Manipulation planning with caging grasps," in *Humanoid Robots, 2008. Humanoids 2008. 8th IEEE-RAS International Conference on*. IEEE, 2008, pp. 285–292.

[24] C. Ferrari and J. Canny, "Planning optimal grasps," in *Proc. IEEE Int. Conf. Robotics and Automation (ICRA)*, 1992, pp. 2290–2295.

[25] D. Fischinger, A. Weiss, and M. Vincze, "Learning grasps with topographic features," *Int. J. Robotics Research (IJRR)*, p. 0278364915577105, 2015.

[26] J. E. Godoy, I. Karamouzas, S. J. Guy, and M. Gini, "Adaptive learning for multi-agent navigation," in *Proceedings of the 2015 International Conference on Autonomous Agents and Multiagent Systems*. International Foundation for Autonomous Agents and Multiagent Systems, 2015, pp. 1577–1585.

[27] R. Goetschalckx, P. Poupart, and J. Hoey, "Continuous correlated beta processes," in *IJCAI Proceedings-International Joint Conference on Artificial Intelligence*, vol. 22, no. 1. Citeseer, 2011, p. 1269.

[28] K. Y. Goldberg and M. T. Mason, "Bayesian grasping," in *Robotics and Automation, 1990. Proceedings., 1990 IEEE International Conference on*. IEEE, 1990, pp. 1264–1269.

[29] C. Goldfeder and P. K. Allen, "Data-driven grasping," *Autonomous Robots*, vol. 31, no. 1, pp. 1–20, 2011.

[30] C. Goldfeder, M. Ciocarlie, H. Dang, and P. K. Allen, "The columbia grasp database," in *Robotics and Automation, 2009. ICRA'09. IEEE International Conference on*. IEEE, 2009, pp. 1710–1716.

[31] C. Goldfeder, M. Ciocarlie, J. Peretzman, H. Dang, and P. K. Allen, "Data-driven grasping with partial sensor data," in *Intelligent Robots and Systems, 2009. IROS 2009. IEEE/RSJ International Conference on*. IEEE, 2009, pp. 1278–1283.

[32] A. Hannun, C. Case, J. Casper, B. Catanzaro, G. Diamos, E. Elsen, R. Prenger, S. Satheesh, S. Sengupta, A. Coates, *et al.*, "Deep speech: Scaling up end-to-end speech recognition," *arXiv preprint arXiv:1412.5567*, 2014.

[33] A. Herzog, P. Pastor, M. Kalakrishnan, L. Righetti, T. Asfour, and S. Schaal, "Template-based learning of grasp selection," in *Robotics and Automation (ICRA), 2012 IEEE International Conference on*. IEEE, 2012, pp. 2379–2384.

[34] A. Herzog, P. Pastor, M. Kalakrishnan, L. Righetti, J. Bohg, T. Asfour, and S. Schaal, "Learning of grasp selection based on shape-templates," *Autonomous Robots*, vol. 36, no. 1-2, pp. 51–65, 2014.

[35] U. Hillenbrand, M. Roa, *et al.*, "Transferring functional grasps through contact warping and local replanning," in *Intelligent Robots and Systems (IROS), 2012 IEEE/RSJ International Conference on*. IEEE, 2012, pp. 2963–2970.

[36] G. Hitz, A. Gotovos, F. Pomerleau, M.-E. Garneau, C. Pradalier, A. Krause, and R. Y. Siegwart, "Fully autonomous focused exploration for robotic environmental monitoring," in *Robotics and Automation (ICRA), 2014 IEEE International Conference on*. IEEE, 2014, pp. 2658–2664.

[37] K. Hsiao, M. Ciocarlie, and P. Brook, "Bayesian grasp planning," in *ICRA 2011 Workshop on Mobile Manipulation: Integrating Perception and Manipulation*, 2011.

[38] K. Hsiao, L. P. Kaelbling, and T. Lozano-Perez, "Grasping pomdps," in *Robotics and Automation, 2007 IEEE International Conference on*. IEEE, 2007, pp. 4685–4692.

[39] D. Hsu, G. Sánchez-Ante, and Z. Sun, "Hybrid prm sampling with a cost-sensitive adaptive strategy," in *Robotics and Automation, 2005. ICRA 2005. Proceedings of the 2005 IEEE International Conference on*. IEEE, 2005, pp. 3874–3880.

[40] Y. Jiang, S. Moseson, and A. Saxena, "Efficient grasping from rgbd images: Learning using a new rectangle representation," in *Robotics and Automation (ICRA), 2011 IEEE International Conference on*. IEEE, 2011, pp. 3304–3311.

[41] G. Kahn, P. Sujan, S. Patil, S. Bopardikar, J. Ryde, K. Goldberg, and P. Abbeel, "Active exploration using trajectory optimization for robotic grasping in the presence of occlusions."

[42] D. Kappler, J. Bohg, and S. Schaal, "Leveraging big data for grasp planning," in *Robotics and Automation (ICRA), 2015 IEEE International Conference on*. IEEE, 2015, pp. 4304–4311.

[43] A. Kasper, Z. Xue, and R. Dillmann, "The kit object models database: An object model database for object recognition, localization and manipulation in service robotics," *The International Journal of Robotics Research*, vol. 31, no. 8, pp. 927–934, 2012.

[44] B. Kehoe, D. Berenson, and K. Goldberg, "Estimating part tolerance bounds based on adaptive cloud-based grasp planning with slip," in *Proc. IEEE Conf. on Automation Science and Engineering (CASE)*. IEEE, 2012, pp. 1106–1113.

[45] ——, "Toward cloud-based grasping with uncertainty in shape: Estimating lower bounds on achieving force closure with zero-slip push grasps," in *Proc. IEEE Int. Conf. Robotics and Automation (ICRA)*. IEEE, 2012, pp. 576–583.

[46] J. Kim, K. Iwamoto, J. J. Kuffner, Y. Ota, and N. S. Pollard, "Physically-based grasp quality evaluation under uncertainty," in *Proc. IEEE Int. Conf. Robotics and Automation (ICRA)*. IEEE, 2012, pp. 3258–3263.

[47] A. Krizhevsky, I. Sutskever, and G. E. Hinton, "Imagenet classification with deep convolutional neural networks," in *Advances in neural information processing systems*, 2012, pp. 1097–1105.

[48] O. Kroemer, R. Detry, J. Piater, and J. Peters, "Combining active learning and reactive control for robot grasping," *Robotics and Autonomous Systems*, vol. 58, no. 9, pp. 1105–1116, 2010.

[49] T. L. Lai and H. Robbins, "Asymptotically efficient adaptive allocation rules," *Advances in applied mathematics*, vol. 6, no. 1, pp. 4–22, 1985.

[50] M. Laskey, J. Mahler, Z. McCarthy, F. Pokorny, S. Patil, J. van den Berg, D. Kragic, P. Abbeel, and K. Goldberg, "Multi-arm bandit models for 2d sample based grasp planning with uncertainty." in *Proc. IEEE Conf. on Automation Science and Engineering (CASE)*. IEEE, 2015.

[51] M. Lauri and R. Ritala, "Optimal sensing via multi-armed bandit relaxations in mixed observability domains," in *Robotics and Automation, 2015. ICRA 2015. Proceedings of the 2005 IEEE International Conference on*. IEEE, 2015.

[52] Q. V. Le, D. Kamm, A. F. Kara, and A. Y. Ng, "Learning to grasp objects with multiple contact points," in *Robotics and Automation (ICRA), 2010 IEEE International Conference on*. IEEE, 2010, pp. 5062–5069.

[53] I. Lenz, H. Lee, and A. Saxena, "Deep learning for detecting robotic grasps," *The International Journal of Robotics Research*, vol. 34, no. 4-5, pp. 705–724, 2015.

[54] B. León, S. Ulbrich, R. Diankov, G. Puche, M. Przybylski, A. Morales, T. Asfour, S. Moisio, J. Bohg, J. Kuffner, *et al.*, "Opengrasp: a toolkit for robot grasping simulation," in *Simulation, Modeling, and Programming for Autonomous Robots*. Springer, 2010, pp. 109–120.

[55] B. Li, Y. Lu, C. Li, A. Godil, T. Schreck, M. Aono, M. Burtscher, Q. Chen, N. K. Chowdhury, B. Fang, *et al.*, "A comparison of 3d shape retrieval methods based on a large-scale benchmark supporting multimodal queries," *Computer Vision and Image Understanding*, vol. 131, pp. 1–27, 2015.

[56] Y. Li and N. S. Pollard, "A shape matching algorithm for synthesizing humanlike enveloping grasps," in *Humanoid Robots, 2005 5th IEEE-RAS International Conference on*. IEEE, 2005, pp. 442–449.

[57] J. Mahler, S. Patil, B. Kehoe, J. van den Berg, M. Ciocarlie, P. Abbeel, and K. Goldberg, "Gp-gpis-opt: Grasp planning under shape uncertainty using gaussian process implicit surfaces and sequential convex programming," 2015.

[58] R. Marchant and F. Ramos, "Bayesian optimisation for intelligent environmental monitoring," in *Intelligent Robots and Systems (IROS), 2012 IEEE/RSJ International Conference on*. IEEE, 2012, pp. 2242–2249.

[59] P. Matikainen, P. M. Furlong, R. Sukthankar, and M. Hebert, "Multi-armed recommendation bandits for selecting state machine policies for robotic systems," in *Robotics and Automation (ICRA), 2013 IEEE International Conference on*. IEEE, 2013, pp. 4545–4551.

[60] A. K. B. R. M. Michalik and B. T. R. Detry, "G3db: A database of successful and failed grasps with rgb-d images, point clouds, mesh models and gripper parameters."

[61] A. T. Miller and P. K. Allen, "Graspit! a versatile simulator for robotic grasping," *Robotics & Automation Magazine, IEEE*, vol. 11, no. 4, pp. 110–122, 2004.

[62] L. Montesano and M. Lopes, "Active learning of visual descriptors for grasping using non-parametric smoothed beta distributions," *Robotics and Autonomous Systems*, vol. 60, no. 3, pp. 452–462, 2012.

[63] F. T. Pokorny, Y. Bekiroglu, and D. Kragic, "Grasp moduli spaces and spherical harmonics," in *Robotics and Automation (ICRA), 2014 IEEE International Conference on*. IEEE, 2014, pp. 389–396.

[64] F. T. Pokorny, K. Hang, and D. Kragic, "Grasp moduli spaces." in *Robotics: Science and Systems*, 2013.

[65] D. Prattichizzo and J. C. Trinkle, "Grasping," in *Springer handbook of robotics*. Springer, 2008, pp. 671–700.

[66] D. Rao, Q. V. Le, T. Phoka, M. Quigley, A. Sudsang, and A. Y. Ng, "Grasping novel objects with depth segmentation," in *Intelligent Robots and Systems (IROS), 2010 IEEE/RSJ International Conference on*. IEEE, 2010, pp. 2578–2585.

[67] C. Rasmussen and C. Williams, *Gaussian processes for machine learning*. MIT Press, 2006.

[68] J. Redmon and A. Angelova, "Real-time grasp detection using convolutional neural networks," *arXiv preprint arXiv:1412.3128*, 2014.

[69] E. Rimon and A. Blake, "Caging 2d bodies by 1-parameter two-fingered gripping systems," in *Robotics and Automation, 1996. Proceedings., 1996 IEEE International Conference on*, vol. 2. IEEE, 1996, pp. 1458–1464.

[70] H. Robbins, "Some aspects of the sequential design of experiments," in *Herbert Robbins Selected Papers*. Springer, 1985, pp. 169–177.

[71] A. Rodriguez, M. T. Mason, and S. Ferry, "From caging to grasping," *Int. J. Robotics Research (IJRR)*, p. 0278364912442972, 2012.

[72] A. Saxena, J. Driemeyer, and A. Y. Ng, "Robotic grasping of novel objects using vision," *The International Journal of Robotics Research*, vol. 27, no. 2, pp. 157–173, 2008.

[73] A. Singh, J. Sha, K. S. Narayan, T. Achim, and P. Abbeel, "Bigbird: A large-scale 3d database of object instances," in *Robotics and Automation (ICRA), 2014 IEEE International Conference on*. IEEE, 2014, pp. 509–516.

[74] T. Stouraitis, U. Hillenbrand, and M. A. Roa, "Functional power grasps transferred through warping and replanning," in *Robotics and Automation (ICRA), 2015 IEEE International Conference on*. IEEE, 2015, pp. 4933–4940.

[75] F. Stulp, E. Theodorou, J. Buchli, and S. Schaal, "Learning to grasp under uncertainty," in *Robotics and Automation (ICRA), 2011 IEEE International Conference on*. IEEE, 2011, pp. 5703–5708.

[76] M. Vahedi and A. F. van der Stappen, "Caging polygons with two and three fingers," *Int. J. Robotics Research (IJRR)*, vol. 27, no. 11-12, pp. 1308–1324, 2008.

[77] W. Wan, R. Fukui, M. Shimosaka, T. Sato, and Y. Kuniyoshi, "Grasping by caging: A promising tool to deal with uncertainty," in *IEEE Int. Conf. on Robotics and Automation (ICRA)*, 2012, pp. 5142–5149.

[78] J. Weisz and P. K. Allen, "Pose error robust grasping from contact wrench space metrics," in *Robotics and Automation (ICRA), 2012 IEEE International Conference on*. IEEE, 2012, pp. 557–562.

[79] W. Wohlkinger, A. Aldoma, R. B. Rusu, and M. Vincze, "3dnet: Large-scale object class recognition from cad models," in *Robotics and Automation (ICRA), 2012 IEEE International Conference on*. IEEE, 2012, pp. 5384–5391.

[80] Y. Zheng and W.-H. Qian, "Coping with the grasping uncertainties in force-closure analysis," *Int. J. Robotics Research (IJRR)*, vol. 24, no. 4, pp. 311–327, 2005.